

## Supplementary Methods

### Methods

#### *Cell lines and Drug Treatment*

All cell lines underwent a standard procedure for detecting mycoplasma and identifying STR. MeiSenCTCC (Zhejiang, China) provided the gastric cancer cell lines used in this research, which included SNU668, KATO-III, NUGC3, MKN45, MKN74, and SNU638 cells. The cells were grown in RPMI1640 (Gibco) with the addition of 10% fetal bovine serum (China, Zhejiang MeiSenCTCC) and 1% penicillin-streptomycin (Gibco). TargetMol (Boston, MA, USA) provided the following compounds: Nut (dissolved in *DMSO*), Ida (dissolved in *DMSO*), Ada (dissolved in *DMSO*), Pf (dissolved in *DMSO*), and MG132(dissolved in *DMSO*).

#### *Fluorescence in situ hybridization*

Before hybridization, the tissue from SRCC and other forms of stomach adenocarcinoma underwent treatment using the Paraffin Pretreatment Reagent Kit protocol (Vysis, IL, USA).The probe combinations utilized were *MDM2* (SpectrumOrange) and centromere 12 (CEP 12 SpectrumGreen).Prior to hybridization, the sections underwent dewaxing, air drying, and dehydration, followed by denaturation for a duration of 5 minutes.Following an overnight hybridization process in a humidification chamber set at 37°C, the slides underwent washing and counterstaining procedures.For every tumor, the calculation was performed to determine the copy numbers of the dominant gene and centromere, considering gene amplification as a ratio of oncogene/centromere  $\geq 2.0$ .

#### **Examinations of cellular viability, growth, and flow cytometry**

A concentration of 1000 cells per well was introduced into 96-well plates, and the viability and growth of the cells were evaluated using the CellTiter-Glo assay for luminescent cell viability (Promega) and BioTek Instruments. The combination index (CI) values were interpreted as follows: CI < 1 indicated synergism, CI = 1 indicated

additivity, and  $CI > 1$  indicated antagonism [1]. The measurement of the cell cycle involved staining with propidium iodide (PI) (Sigma-aldridge) for a duration of 30 minutes. Subsequently, analysis was conducted utilizing CytoFLEX (Beckman) and Cytexpert (Beckman) software.

### **Colony formation assay**

After digesting and counting the cells, 20,000 cells were inoculated into each well of a 6-well plate, and the culture medium was renewed every three days for a total of 12 days. Afterwards, the colonies underwent PBS rinsing, fixation with 4% paraformaldehyde, more PBS rinsing, staining with 0.1% crystal violet for half an hour, followed by additional PBS rinsing, drying, and imaging with a ChemiDoc MP imager (BioRad).

### ***Tumorsphere formation assay***

Each well of a 12-well ultra-low adhesion plate contained 10,000 cells that were evenly dispersed. In order to preserve the integrity of the tumor spheres, 500 microliters of the same solution were supplemented every three days. Following a 10-day period of incubation, the spheres were captured in photographs and then underwent semi-quantitative analysis of tumor ball formation using ImageJ software, which is based in Maryland, USA.

### ***Real-Time Quantitative PCR***

The cells were subjected to total RNA extraction using the TRIzol kit (R401-01, Vazyme) as per the guidelines provided by the manufacturer [2]. DNase I, GMP Grade (Cat. No.: GMP-E127) which provides by Novoprotein (Shanghai, China) was used to eliminate the contamination of DNA. The TransStart® Top Green qPCR SuperMix Kit (Transgen, Beijing, China) was utilized for conducting reverse transcription. The Light-Cycler 480 system (Roche) was utilized for QPCR, following the previously described method [3]. To achieve the normalization of target gene expression levels, the corresponding 18S threshold cycle (Ct) value was subtracted. The primer sequences are

included in Supplementary Table4.

### ***Western blot***

The BCA method was used to lyse, sonicate, and quantify the cells. The same amount of protein was isolated using SDS-PAGE and then transferred onto a polyvinylidene fluoride membrane with a pore size of 0.45 $\mu$ m. The western blot was visualized using the ChemiDoc MP imager of BioRad. In this study, a range of primary antibodies were used, including anti-MDM2 (1:500; 27883-1-AP, Proteintech), anti-E-cadherin (1:1000; #14472, CST), anti-N-cadherin (1:500; sc-8424, Santa Cruz), anti-p53 (1:500; sc-126, Santa Cruz), anti-Phospho-Histone H2A.X (Ser139) (1:1000; #2577, CST), anti-RAD51 (1:500; sc-398587, Santa Cruz), and anti-ubiquitin (1:1,000; Proteintech, 10201-2-ap).  $\beta$ -Actin served as the loading control. Colormixed protein marker was applied as a protein size marker (M221-01, GenStar). The immunoblotting analysis of the membranes was performed using ECL Western Blotting Substrate (MK-S400, MIKX, Shenzhen, China).

### ***Co-IP analysis***

After performing cell counting, a total of 10 million cells were placed in a culture dish with a diameter of 10cm. Cells were treated with Nut (10 $\mu$ M) before assessing ubiquitination levels. Afterwards, the lysates of the cells were incubated with a particular primary antibody, specifically anti-MDM2 (1:200; Cat# sc-965, Santa Cruz) and anti-E-cadherin (1:200; Cat# sc-8426, Santa Cruz). Then, they were mixed with protein A/G-Sepharose beads (Thermo Scientific Pierce) and left overnight at 4C. Following a comprehensive wash, the magnetic beads were treated with 3X SDS-PAGE loading buffer (Cat#7722, CST) and heated for 5 minutes. Subsequently, a specific antibody was utilized for western blot analysis to identify the protein complex.

### ***Immunofluorescence staining***

To start, the confocal dish was emptied of the liquid on top and rinsed with PBS three times. Then, cells or tissues were immediately fixed with 4% paraformaldehyde for 15

minutes and washed with PBS three times. After permeating the cell membrane, the primary antibody was incubated and left overnight at 4°C. Afterwards, the subsequent antibody, labeled with Alexa Fluor 488, was thoroughly washed at room temperature prior to incubation with 40,6-diamidino-2-phenylindole diluted in methanol for 10 minutes. Images were acquired using fluorescence and laser confocal microscopes from ZEISS, and the ZEISS (Carl Zeiss, Thornwood) software system was used to semi-quantitatively evaluate the fluorescence intensity of Phospho-Histone H2A.X (Ser139).

### ***IHC staining***

The tissues collected from individuals with gastric cancer, surrounding healthy regions, and xenotransplantation tumors were preserved and interred. The tumor tissues from humans were immobilized with formalin for at least 12 hours. The tumor tissues from mice were immobilized with 4% paraformaldehyde. MDM2 (Zsbio, ZM-0425), E-cadherin (Zsbio, ZM-0092), Ki67 (Zsbio, ZM-0167), cleaved caspase-3 (1:200, Cell Signaling Technology, #9661), p53 (1:50; sc-126, Santa Cruz) and Phospho-cdc2 (Tyr15) (1:50, Cell Signaling Technology, #9111) expression levels were determined using Immunohistochemical (IHC) staining. Microscopic images were obtained with an Olympus microscope (BX51). Slides were treated with polymer anti-rabbit or anti-mouse antibodies labeled with horseradish peroxidase. The immunohistochemical scores of tissues derived from humans were acquired by consulting literature [4]. A previously described technique [5] was used to quantify the histopathologic score of the mouse stomach.

### ***Mice Experiments***

Female athymic BALB/c nude mice (5-8 weeks old) obtained from GemPharmatech CO., Ltd (China) were housed in a high-quality animal laboratory with SPF-grade conditions. In the right flank,  $5 \times 10^6$  SNU668 and NUGC3 cells were implanted into the mice via subcutaneous injection. Upon reaching a tumor size of 50 mm<sup>3</sup>, randomization was conducted by equally distributing mice with similar tumor burdens into different groups. During the pharmaceutical tests with Ida, SNU668 xenograft mice

were given DMSO, Ida (n=7, 37.5 mg/kg, oral gavage(i.g.) every three days), Ada (n=7, 150 mg/kg, i.g. every three days), and a mixture of both substances with the same dosage (n=7). NUGC3 xenograft mice were given DMSO, Ida (n=8, 37.5 mg/kg, i.g. every three days), Ada (n=8, 150 mg/kg, i.g. every three days), and a combination of both substances with the same dosage (n=8) during the study. To conduct the pharmaceutical trials of Nut,  $5 \times 10^6$  NUGC3 cells were implanted into the mice's flank through subcutaneous means. Mice with similar tumor load were divided into four groups: mice treated with DMSO (n=4, i.g., every three days), Nut (n=4, 50 mg/kg, intraperitoneal injection (i.p.) every three days), Ada (n=4, 150 mg/kg, i.g. every three days), and combination of both compounds at the same dose (n = 4). The advancement of the tumor was assessed by monitoring its overall weight and size on alternate days. After The tumors were measured using a Vernier caliper and their volume was calculated using the following formula:  $V = W^2 \times L/2$ . To illustrate the absorption of Ida and Ada, liquid chromatography mass spectrometry (LC-MS) was performed to assess the drug concentration of plasma from BALB/c nude mice which were treated by Ida (n=3), Ada (n=3) and DMSO (n=6) for 3 hours, respectively. This study included all experimental samples, except for one mouse in the combination treatment group that succumbed to an unexpected illness. The tumors were monitored for about three weeks following administration of the medication and were excised either when they reached a volume of 1500 mm<sup>3</sup> or at the end of the investigation. Blood samples were collected from Female athymic BALB/c nude mice during in vivo studies to determine the plasma concentrations of Ada and Ida. Samples were collected at 3 hours after the first dose in each treatment group, which consisted of Ada at 150 mg/kg and Ida at 37.5 mg/kg. Pharmacokinetic assessment was conducted using noncompartmental analysis with Analyst 1.6.3 (AB Sciex) [6, 7]. The animal experiments followed the animal experiment plan that was approved by the Animal Protection and Ethics Committee of Sun Yat-sen University (SYSU-IACUC-2022050601), and they were conducted in accordance with the national health guidelines for animal protection and use.

### ***Organoid Culture***

Tumor tissues from the stomach were obtained from The Sixth Affiliated Hospital of Sun Yat-sen University after receiving informed consent and ethical approval from the SYSU-IACUC-2020-000570 committee, with the approval code 2021ZSLYEC-325. Afterwards, the tissue block was finely chopped and moved to a dissociation tube filled with digestive juice for tissues. The Tumor Dissociation Kit (Miltenyi Biotec, 130-095-929) was used to dissociate fresh tumor tissues into single-cell suspensions. To stop digestion, a digestion termination solution was introduced, followed by centrifugation, and then removing the supernatant. The culture of SRGC organoids was conducted utilizing GC organoid medium, as previously documented [8].

### ***Clinical Samples and Database***

From January 2013 to August 2022, a total of 294 patients who had undergone primary radical resection for GC provided paraffin-embedded pathological specimens for this study as The Sixth Affiliated Hospital of Sun Yat-sen University (SYSU) cohort. The follow-up office's GC database included clinicopathological variables, which covered general details, pathological categorization, and follow-up outcome information. The evaluation of tumor pT, pN, and PM status was conducted based on the stage criteria of the American Joint Committee on Cancer (AJCC) Seventh Edition [9]. The clinicopathological data collection was authorized by the Institutional Review Board (IRB) of the Sixth Affiliated Hospital, Sun Yat-sen University, with the approval code 2021ZSLYEC-325. The main objective of the research was to assess the overall survival (OS) rate, which refers to the period from diagnosis to decease. The GEPIA database ([GEPIA 2 \(cancer-pku.cn\)](http://cancer-pku.cn)), Kaplan-Meier Plotter database ([Kaplan-Meier plotter \[Gastric\] \(kmplot.com\)](http://Kaplan-Meier_plotter[Gastric](kmplot.com))), Cbioportal database ([cBioPortal for Cancer Genomics](http://cBioPortal for Cancer Genomics)) and CCLE database ([Datasets | Cancer Cell Line Encyclopedia \(CCLE\) \(broadinstitute.org\)](http://Datasets|Cancer Cell Line Encyclopedia (CCLE) (broadinstitute.org))) were used in this study [10-13].

### ***Statistical analysis***

GraphPad Prism 9.0(GraphPad Prism Software, Inc.) was utilized for the statistical analysis of the data, employing Student's t-test to ascertain the disparities between the

two groups. Moreover, a two-way analysis of variance (ANOVA) was employed to determine the statistical difference in the dose-response curves, as indicated in the captions of the figures. The data reported represents the average  $\pm$  standard deviation of three separate trials. Statistical tests were considered statistically significant if the P-value was less than 0.05, unless otherwise specified. The data shows statistical significance as follows: \*,  $P < 0.05$ ; \*\*,  $P < 0.01$ ; \*\*\*,  $P < 0.001$ .

## Reference

1. Chou TC: **Drug combination studies and their synergy quantification using the Chou-Talalay method.** *Cancer Res* 2010, **70**(2):440-446.
2. Wu W, Li K, Zhao H, Xu X, Xu J, Luo M, Xiao Y, Tian L: **Tip60 Phosphorylation at Ser 99 Is Essential for Autophagy Induction in Bombyx mori.** *Int J Mol Sci* 2020, **21**(18).
3. Jégu T, Blum R, Cochrane JC, Yang L, Wang CY, Gilles ME, Colognori D, Szanto A, Marr SK, Kingston RE, Lee JT: **Xist RNA antagonizes the SWI/SNF chromatin remodeler BRG1 on the inactive X chromosome.** *Nat Struct Mol Biol* 2019, **26**(2):96-109.
4. Yu Z, Deng P, Chen Y, Liu S, Chen J, Yang Z, Chen J, Fan X, Wang P, Cai Z *et al*: **Inhibition of the PLK1-Coupled Cell Cycle Machinery Overcomes Resistance to Oxaliplatin in Colorectal Cancer.** *Adv Sci (Weinh)* 2021, **8**(23):e2100759.
5. Prasad K, Prabhu GK: **Image analysis tools for evaluation of microscopic views of immunohistochemically stained specimen in medical research-a review.** *J Med Syst* 2012, **36**(4):2621-2631.
6. Chen L, Pastorino F, Berry P, Bonner J, Kirk C, Wood KM, Thomas HD, Zhao Y, Daga A, Veal GJ *et al*: **Preclinical evaluation of the first intravenous small molecule MDM2 antagonist alone and in combination with temozolomide in neuroblastoma.** *Int J Cancer* 2019, **144**(12):3146-3159.
7. Takebe N, Naqash AR, O'Sullivan Coyne G, Kummar S, Do K, Bruns A, Juwara L, Zlott J, Rubinstein L, Piekarz R *et al*: **Safety, Antitumor Activity, and Biomarker Analysis in a Phase I Trial of the Once-daily Wee1 Inhibitor Adavosertib (AZD1775) in Patients with Advanced Solid Tumors.** *Clin Cancer Res* 2021, **27**(14):3834-3844.
8. Yamaguchi K, Yoshihiro T, Ariyama H, Ito M, Nakano M, Semba Y, Nogami J, Tsuchihashi K, Yamauchi T, Ueno S *et al*: **Potential therapeutic targets discovery by transcriptome analysis of an in vitro human gastric signet ring carcinoma model.** *Gastric Cancer* 2022, **25**(5):862-878.
9. Ajani JA, D'Amico TA, Bentrem DJ, Chao J, Cooke D, Corvera C, Das P, Enzinger PC, Enzler T, Fanta P *et al*: **Gastric Cancer, Version 2.2022, NCCN Clinical Practice Guidelines in Oncology.** *J Natl Compr Canc Netw* 2022, **20**(2):167-192.
10. Szász AM, Lánczky A, Nagy Á, Förster S, Hark K, Green JE, Boussioutas A, Busuttill R, Szabó A, Gyórfy B: **Cross-validation of survival associated biomarkers in gastric cancer using transcriptomic data of 1,065 patients.** *Oncotarget* 2016, **7**(31):49322-49333.
11. Tang Z, Kang B, Li C, Chen T, Zhang Z: **GEPIA2: an enhanced web server for large-scale**

- expression profiling and interactive analysis.** *Nucleic Acids Res* 2019, **47**(W1):W556-w560.
12. Cerami E, Gao J, Dogrusoz U, Gross BE, Sumer SO, Aksoy BA, Jacobsen A, Byrne CJ, Heuer ML, Larsson E *et al*: **The cBio cancer genomics portal: an open platform for exploring multidimensional cancer genomics data.** *Cancer Discov* 2012, **2**(5):401-404.
  13. Barretina J, Caponigro G, Stransky N, Venkatesan K, Margolin AA, Kim S, Wilson CJ, Lehár J, Kryukov GV, Sonkin D *et al*: **The Cancer Cell Line Encyclopedia enables predictive modelling of anticancer drug sensitivity.** *Nature* 2012, **483**(7391):603-607.

## Supplementary Figures

### Supplementary Figures

**Figure S1. Copy number gains of *MDM2* are a critical characteristic of SRCC and high *MDM2* expression correlates with poor prognosis** (A and B) Kaplan-Meier survival curves of overall survival (OS) time (A) and disease-free survival (DFS) time (B) of Asian cancer research group (ACRG) cohort of gastric cancer according to signet ring cell carcinoma (SRCC) (red, n = 41) and another type (non-SRCC) (blue, n = 257). (C and D) Kaplan-Meier survival curves of OS time (C) and progression-free survival (PFS) time (D) in TCGA cohort of gastric cancer according to SRCC (red, n = 13) and another type (non-SRCC) (blue, n = 403). (E) Quantification of *MDM2* expression in carcinoma (red, n = 297) and adjacent tissue (n = 302) of the stomach from the SYSU TMA cohort. (F) The mRNA expression of *MDM2* of carcinoma (red, n=408) and adjacent tissue (blue, n=211) of the stomach from the TCGA cohort. (G) Kaplan-Meier survival curves of PFS time from Kaplan-Meier Plotter Database according to high (red, n = 130) and low (blue, n = 368) *MDM2* expression. (H) Genetic alteration frequency of *MDM2* of GI-tract adenocarcinoma (stomach adenocarcinoma and colorectal adenocarcinoma) in TCGA-Pancancer Atlas. (I) Genetic alteration frequency of *MDM2* of stomach adenocarcinoma in TCGA cohort.

**Figure S2 Inhibition of *MDM2* suppresses E-cadherin degradation in SRCC cells independent of *TP53* status** (A) Representative image of tumor sphere formation assay in gastric cancer cells treated with Nut and Ida after 10 days of cell culture (Scale bar, 200  $\mu$ m). (B) The tumor sphere semi-quantitative histogram of SNU668, KATOIII,



MKN45 and AGS cells treated by Nut and Ida. (C and D) The protein levels (C) and mRNA levels (D) of MDM2 expression in gastric cancer cell lines. (E) Efficacy of MDM2 inhibitors (Idasanutlin (Ida) 2.5  $\mu$ M; Amg-232, 10  $\mu$ M) in gastric cancer cell lines from CCLE database. (F) The cell cycle analysis on NUGC3 treated with Nut for 48h. Left panel, representative images of fluorescence-activated cell sorting (FACS) analysis, right panel, S-G2/M phase.

**Figure S3. Inhibition of MDM2 suppress E-cadherin degradation in SRCC cells independent of *TP53* status** (A) The frequency of *MDM2* amplification was investigated in gastric cancer, ESCA, COAD, BC, PC, OV, ATC and Pan-cancer based on the *TP53* mutation status or wild-type status. ESCA, Esophageal Cancer; COAD, Colon Cancer; BC, Breast Cancer; PC, Pancreatic Cancer; OV, Ovarian Cancer; ATC, Anaplastic Thyroid Cancers. (B) The Kaplan-Meier curves depicting the progression-free survival time of STAD, GBM, BLCA, BRCA, PAAD and ESCA in the TCGA cohort were stratified based on *TP53* status and *MDM2* mRNA expression level. STAD, Stomach adenocarcinoma; GBM, Glioblastoma multiforme; BLCA, Bladder Urothelial Carcinoma; BRCA, Breast invasive carcinoma; PAAD, Pancreatic adenocarcinoma; ESCA, Esophageal carcinoma.

**Figure S4. Inhibition of MDM2 suppress E-cadherin degradation in SRCC cells independent of *TP53* status** (A and C) The correlation between the copy number of *MDM2* (A), expression of MDM2 (B) and E-cadherin (C) and the sensitivity of MDM2i (MDM2 inhibitors) (Nut, Ida and RG7338) of all cancer cell lines from Cancer Dependency Map Database (<https://depmap.org/portal/>).

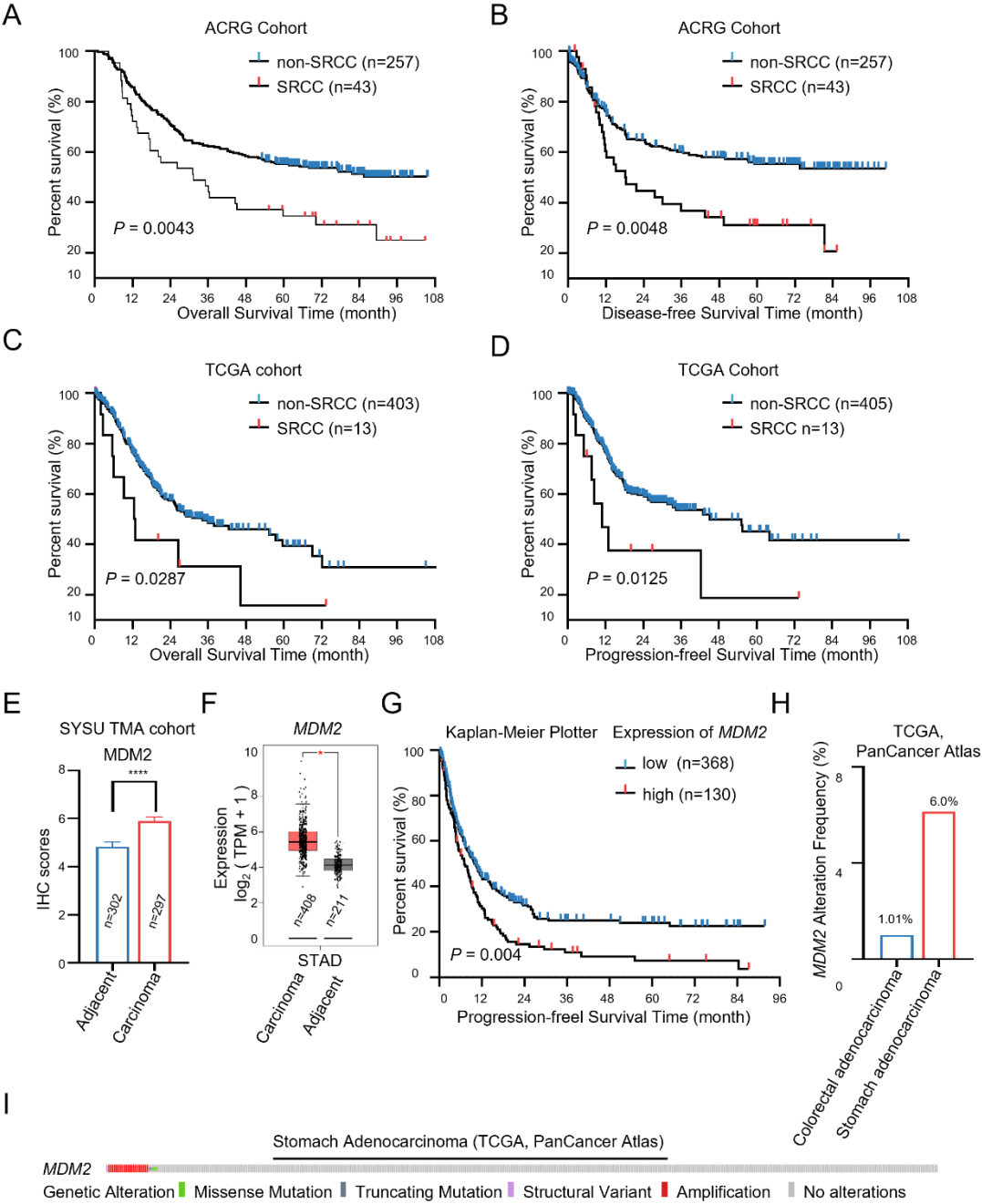
**Figure S5. Combined MDM2 inhibitors with G2/M checkpoint inhibitors can induce a synergistic antitumor effect on SRCC *in vitro*** (A) The representative image of colony formation assay of SNU668 cells treated with si-*MDM2*. (B) The representative image of cell morphology of SNU668 treated with si-*MDM2* for 72 h (scale bar, 100  $\mu$ m). (C) The protein level of MDM2 expression in SNU668 is

transfected by si-*MDM2*. (D) Upper panel, the representative image of the tumor sphere formation assay in NUGC3 treated with Ida, Ada, Pf, or a combination of these compounds at specified concentrations (Ida 2.5  $\mu$ M, Ada 0.25  $\mu$ M, Pf 0.5  $\mu$ M) for 10 days (Scale bar, 200  $\mu$ m). Lower panel, the relative tumor spheres formation rate. (E) Upper panel, the representative image of the tumor sphere formation assay in SNU668 treated with Ida, Ada, Pf, or a combination of these compounds at specified concentrations (Ida 2.5  $\mu$ M, Ada 0.25  $\mu$ M, Pf 0.1  $\mu$ M) for 10 days (Scale bar, 200  $\mu$ m). Lower panel, the relative tumor spheres formation rate. (F) Relative quantification of  $\gamma$ -H2AX intensity in NUGC3 treated with Nut, Ada, or combination at an indicated concentration (Nut 10  $\mu$ M, Ada 0.25  $\mu$ M, Pf 0.25  $\mu$ M) for 72h. (G) Relative quantification of  $\gamma$ -H2AX intensity in SNU668 treated with Nut, Ada, or combination at an indicated concentration (Nut 10  $\mu$ M, Ada 0.25  $\mu$ M, Pf 0.025  $\mu$ M) for 72h. (H) Quantitative of protein level of SNU668 and NUGC3 cells were subjected to Western blot analysis after treatment with Nut, Ada, Pf, or a combination of these compounds at specified concentrations (Nut 10  $\mu$ M, Ada 0.25  $\mu$ M; Pf 0.025  $\mu$ M for SNU668; Pf 0.25 $\mu$ M for NUGC3) for a duration of 4 hours.

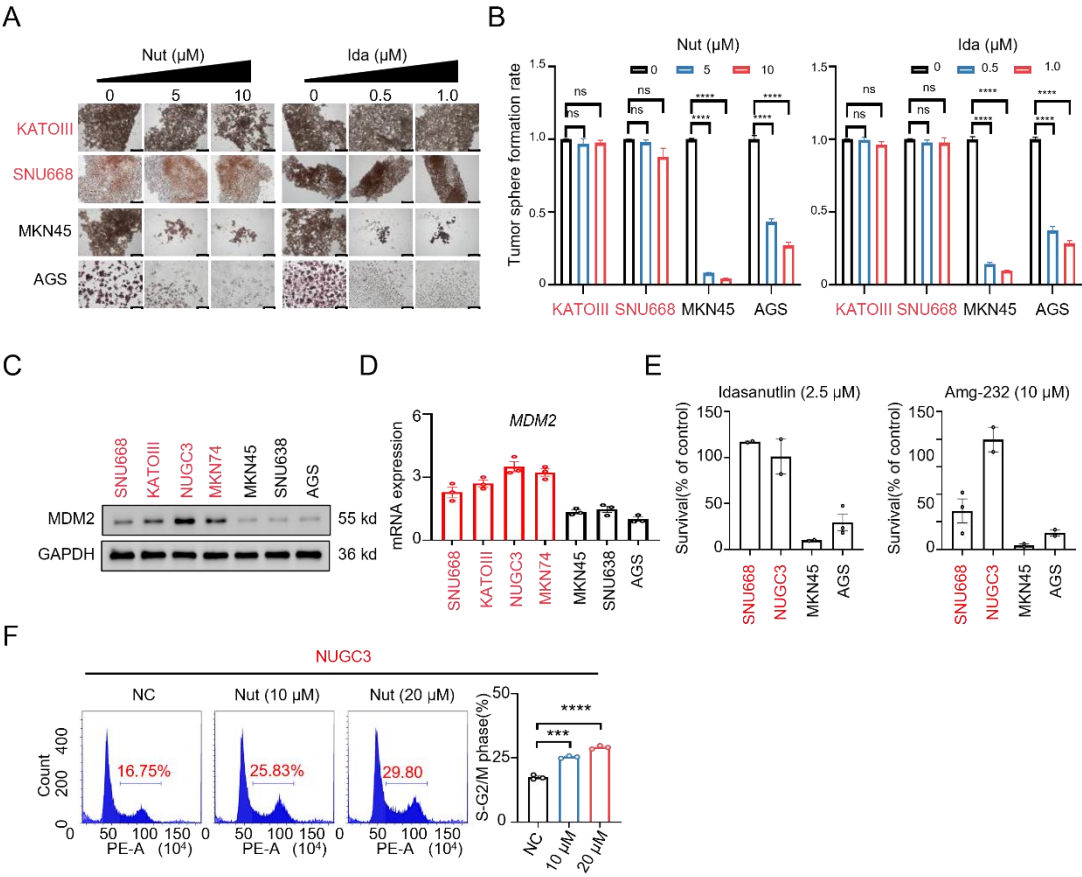
**Figure S6. Combination of MDM2 inhibitor and G2/M checkpoint inhibitors induces a synergistic anti-tumor effect *in vivo*** (A) Pattern: Nut (i.p.,50 mg/kg) or Ida (i.g., 37.5mg/kg), Ada (i.g., 150 mg/kg) alone or in combination following successful modeling of either SNU668 or NUGC3 xenografts. (B) Photograph showing tumor size of NUGC3 xenograft with the treatment of Nut, Ada, and combination of Nut and Ada after 20 days. (C) Tumor weights of NUGC3 xenograft were assessed. (D) Growth curve of tumor volume in vivo efficacy of Nut and Ada in NUGC3 xenograft. (E) The representative image of Ki-67 and cleaved-caspase 3 of IHC in NUGC3 xenografts tumors (Scale bar, 20  $\mu$ m). (F and I) PK analysis of active Ida (n=3) (F) and Ada (n=3) (I) levels using LC–MS in plasma harvested at the 3 hours from a single dose (37.5 mg/kg and 150 mg/kg). (G and H) Extracted ion chromatogram of active Ida (G) and Ada (H). (J and K) Normalized curve of standard sample from Ada (J) and Ida (K). (L) Representative IHC image of MDM2 is staining of tissue and organoids derived from

SRCC-1099 and GC-1097 (Scale bar, 25  $\mu$ m; Scale bar, 50  $\mu$ m).

Figure S1

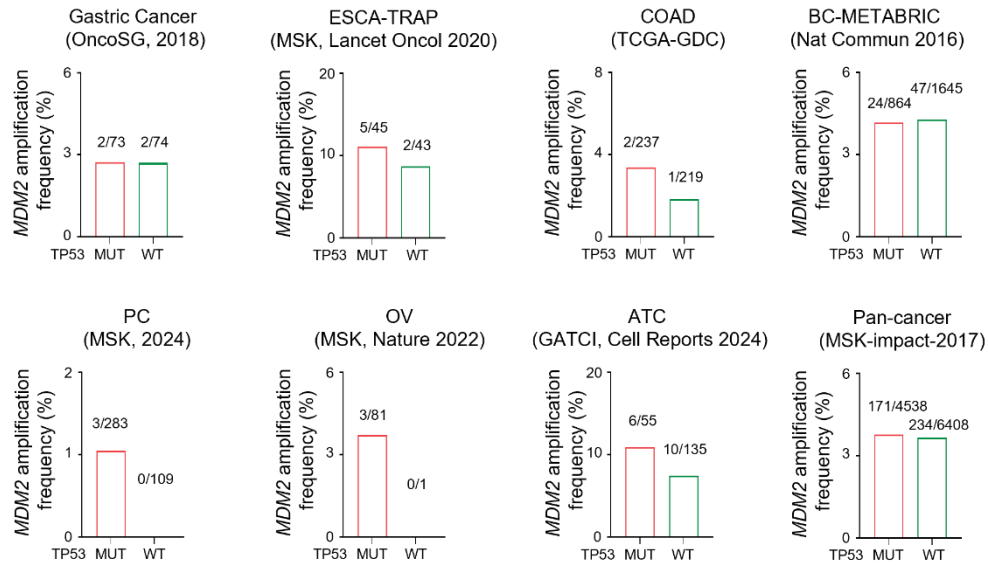


FigureS2



# FigureS3

A



B

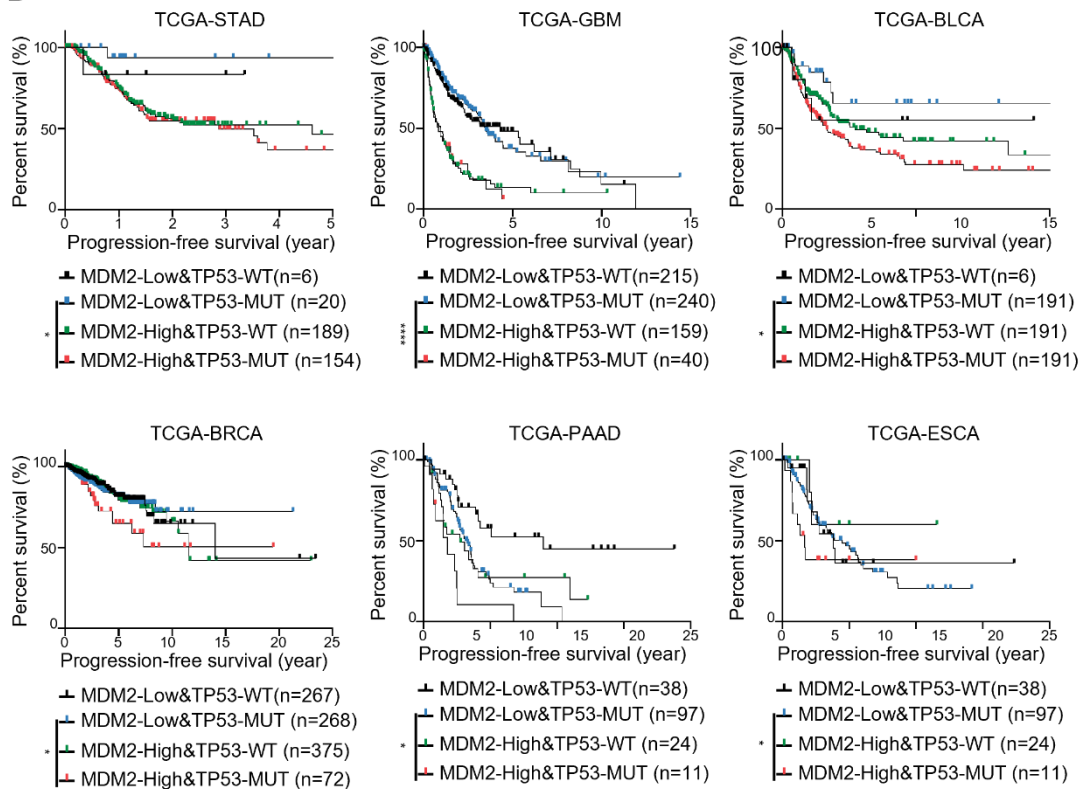
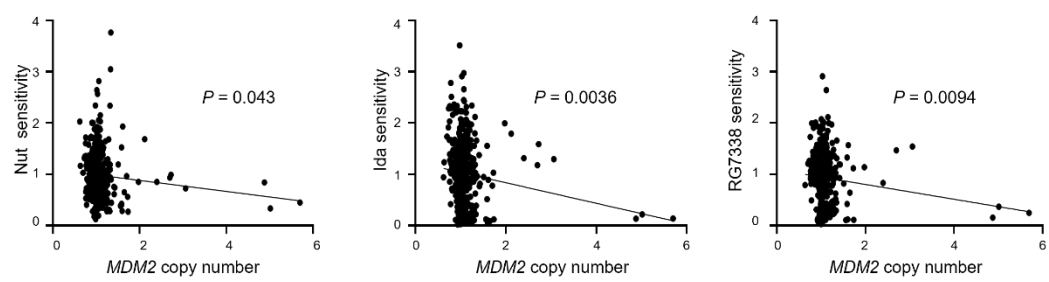
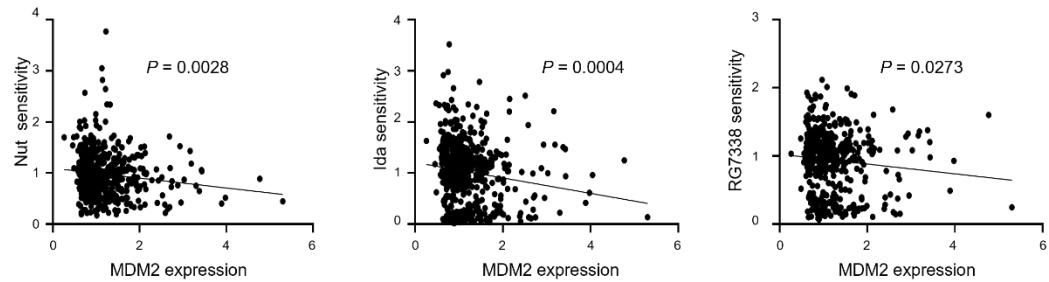


Figure S4

A



B



C

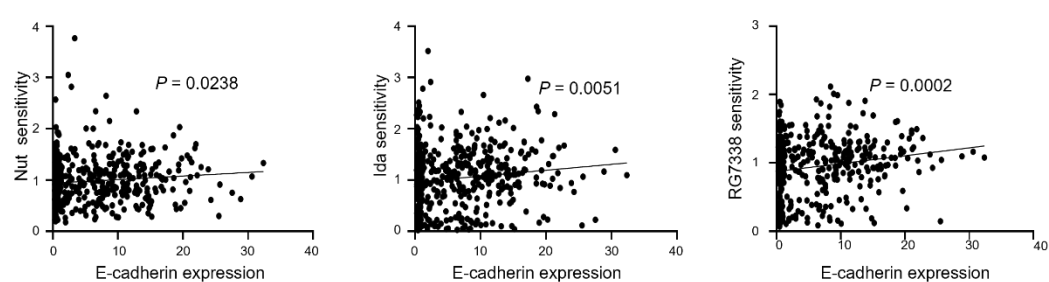


Figure S5

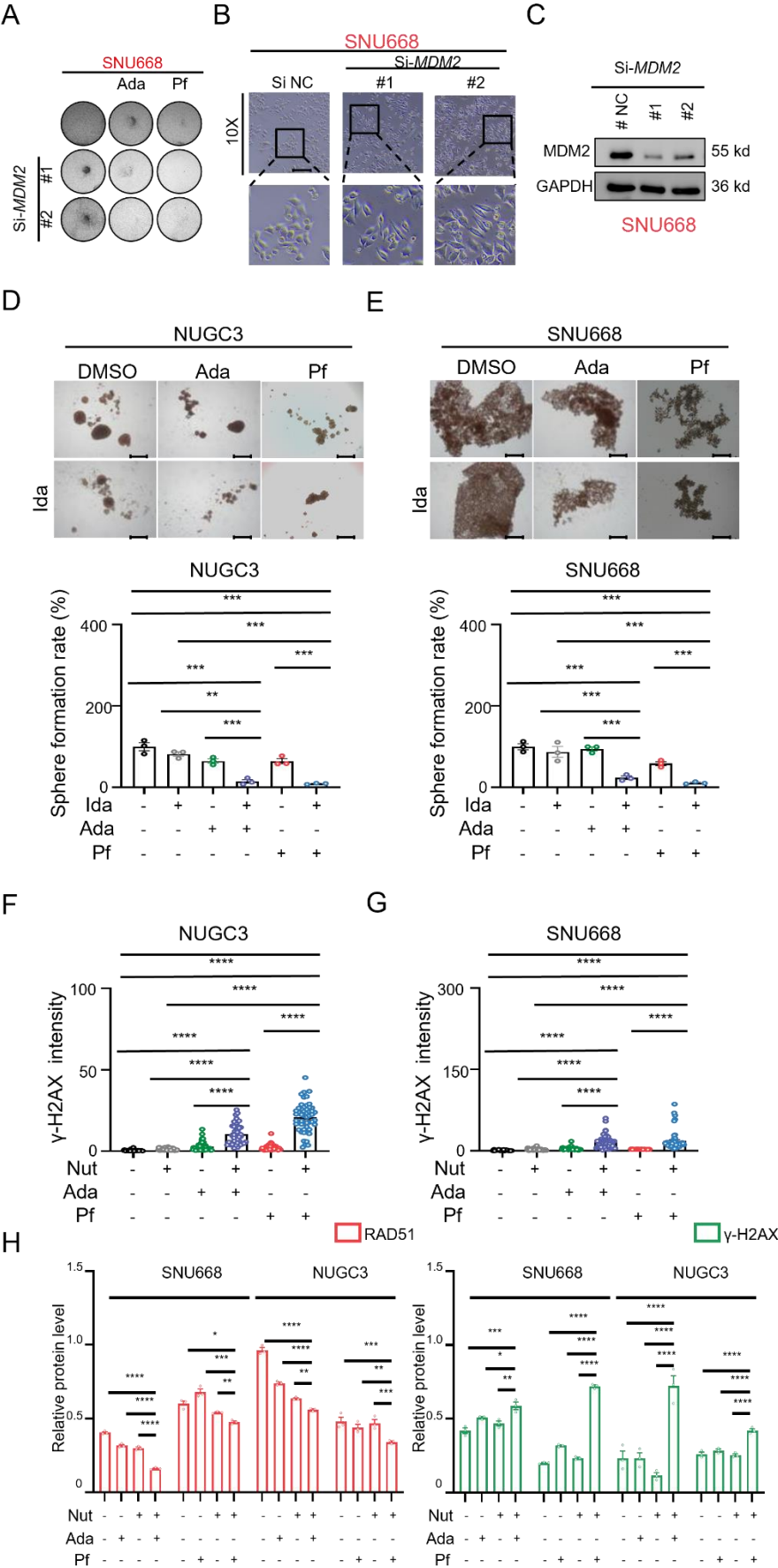


Figure S6

